Available online at www.sciencedirect.com
ScienceDirect
journal homepage: http://www.elsevier.com/locate/acme

Original Research Article

The microstructure and oxidation resistance of the aluminide coatings deposited by the CVD method on pure nickel and hafnium-doped nickel superalloys

M. Zagula-Yavorska [*], *J. Romanowska, M. Pytel, J. Sieniawski*

Department of Materials Science, Rzeszow University of Technology, W. Pola 2 Street, 35-959 Rzeszow, Poland

ARTICLE INFO

Article history:
Received 24 November 2014
Accepted 26 March 2015
Available online 14 April 2015

Keywords:
Coatings
Hafnium
Nickel superalloys
Oxidation

ABSTRACT

Aluminide coating were deposited on pure nickel and hafnium-doped nickel superalloys Mar M247, Mar M200 and CMSX 4 by means of the CVD method. All coatings consisted of two layers: an outer, comprising the β-NiAl phase and the interdiffusion one. The interdiffusion layer on pure nickel consisted of the γ′-Ni_3Al phase and of the NiAl phase on superalloys. MC and $M_{23}C_6$ carbides besides the NiAl phase were found in the interdiffusion zones on Mar M247 and Mar M200, whereas topologically close-packed phases, such as the TCP σ-phase and the R phase were found in the interdiffusion zone on CMSX 4. Coatings on substrates containing more hafnium (Mar M247 and Mar M200) were more resistant to degradation during the cyclic oxidation. The amount of 1.5–1.8 wt.% hafnium in the substrate let to the HfO_2 'pegs' formation in the oxide scale during oxidation of aluminized Mar M247 and Mar M200 superalloys. The improvement of lifetime of coated CMSX 4 superalloy was obtained by platinum modification. Platinum decreased diffusion of alloying elements such as Ti and Ta from the substrate to the coating and oxide scale, stabilized the NiAl phase and delayed the NiAl → Ni_3Al phase transformation.

1. Introduction

Turbine blades used in engine hot sections are made of nickel superalloys and are mainly degraded by high temperature oxidation and hot corrosion phenomena. The application of aluminum as an alloying element in diffusion coatings is an effective way to increase the oxidation and hot corrosion resistance of treated parts. This is obtained by the formation of a protecting surface of Al_2O_3 oxide [1].

Protective aluminide coatings deposited on superalloys are degraded by the loss of Al due to oxidation of the coating surface and the formation of aluminum oxide by interdiffusion of aluminum through the substrate [2]. This process accelerates the rate of the oxide growth and results in the loss of the coating strength and deformation of the coating. Therefore, in order to improve the oxidation resistance of the coating, it is necessary to slow oxide scale growth and improve its adherence [3–6]. Aluminum chemical potential gradient

---

[*] *Corresponding author.* Tel.: +48 178651230.
E-mail address: yavorska@prz.edu.pl (M. Zagula-Yavorska).

http://dx.doi.org/10.1016/j.acme.2015.03.006

between the superalloy and the coating is the driving force of the Al loss. Candidate diffusion barrier materials should retard Al diffusion at high temperatures, possess good thermo-mechanical compatibility with the substrate and the coating and remain relatively stable for extended periods of time at high temperature. The addition of small amount of reactive elements such as: hafnium, zirconium, yttrium and cerium has a beneficial effect on the oxidation behavior of superalloys [7,8]. This beneficial effect includes an improvement of adhesion of alumina scales and the reduction of oxide scale growth rate. Pint et al. [8,9] proved that hafnium doping of β-NiAl and Ni–Pt aluminides reduce the parabolic rate constant by a factor of ten and may be more efficient than platinum doping. Hafnium addition to the nickel superalloy decreases the propensity for rumpling oxides when it diffuses into coating and to the growing aluminum oxide [8,10].

Hafnium is a reactive metal. Its melting temperature is 2225 °C. Hafnium has extremely high chemical reactivity with various elements, for instance oxygen, nitrogen, hydrogen and carbon [8,11]. Some authors [8,12–14] showed, that the small content of hafnium (0.1–1.0 wt.%) improves high temperature mechanical properties of coatings.

Addition of small amount of hafnium (<1 wt.%) to the coating and controlling its level and distribution in aluminide coatings remains an open issue [15].

Warnes et al. [14] and Nesbitt et al. [16] suggest that NiAl-based alloys containing small amount of reactive elements (hafnium or zirconium) added with or in place of platinum results in further improvements of the lifetime. The addition of reactive elements to these alloys causes an improvement of the alumina scale adhesion and the reduction of the growth rate of the scale by the segregation of reactive elements' ions on the scale grain boundaries and alloy-scale interface [17,18]. Research at the SIFCO Company resulted in the development of several new overlay coating and alloys containing 2 at.% hafnium and/or zirconium and up to 5 at.% chromium [8,19]. The oxidation resistance of these coatings was comparable to modern (Ni,Pt) diffusion coatings.

There are a lot of data concerning the deposition of aluminide coatings by pack cementation, EB-PVD and VPA methods [20,21]. But depends on the disposing equipment the technology of the coating deposition process is different. In the available literature there is no data about the aluminization process performed by the CVD method. The technological data are unavailable. Therefore the aim of this work was to produce aluminide coatings using the CVD equipment BPXPR0325S manufactured by IonBond company, examine the microstructure of the coatings deposited on pure nickel and hafnium-doped nickel based superalloys Mar M247, Mar M200 and CMSX 4 and to determine the influence of reactive elements on the oxidation resistance of coated superalloys during air exposure at the high temperature. Examined superalloys are used for high pressure turbine blades in the jet engine made by Pratt & Whitney company and pure nickel was used to analyze the influence of the substrate chemical composition on the coating's microstructure. Moreover new and original contribution of this paper is the investigation of oxidation behavior of coated Mar M200 superalloy containing hafnium, since available experimental data on this subject is scarce. The oxidation resistance of aluminide coatings deposited on hafnium-doped superalloys was compared to the oxidation resistance of the platinum modified aluminide coating deposited on CMSX 4 superalloy.

2. Experimental

The commercial nickel (99.95 wt.% purity), Mar M247 (polycrystal), Mar M200 (directionally solidified crystal) and CMSX 4 (single crystal) superalloys were used as the base material. The chemical composition of the superalloys is given in Table 1.

Cylindrical samples were cut and grounded up to SiC No600, degreased in ethanol, ultrasonically cleaned and finally aluminized. Aluminide coatings were deposited using the CVD equipment BPXPR0325S manufactured by IonBond company (Fig. 1) [3,22–27].

The aluminizing process was conducted at 1050 °C during 8 h in the hydrogen atmosphere. In this process aluminum chloride vapor ($AlCl_3$) was produced in an external generator at 330 °C according to the reaction:

$$2Al + 6HCl \rightarrow 2AlCl_3 + 3H_2 \quad (1)$$

Then $AlCl_3$ was transported in a stream of hydrogen into the CVD reactor, where samples were placed. $AlCl_3$ vapor reacted with nickel, the main constituent of samples and grains of intermetallic phase (NiAl) were formed according to the reaction:

$$2AlCl_3 + 2Ni + 3H_2 \rightarrow 2AlNi + 6HCl \quad (2)$$

The platinum layer (3 μm thick) was deposited in the electroplating process on the CMSX 4 superalloy. Afterwards, the sample was subjected to diffusion treatment at 1050 °C for 2 h under argon atmosphere. The diffusion treated specimen was aluminized by the chemical vapour deposition process.

The microstructure of the surface and cross-sections of the synthesized coatings were investigated by an optical microscope Nikon Epiphot 300, a scanning electron microscope (SEM) Hitachi S-3400N, an energy dispersive spectroscope (EDS) and a scanning-transmission electron microscope STEM

Table 1 – The chemical composition of the investigated superalloys.

Superalloy	Chemical composition, wt.%														
	Ni	Cr	C	Mo	Nb	Ta	Al	Ti	Co	W	Hf	Fe	B	Zr	Re
Mar M247	60.83	8.25	0.15	0.7	–	2.51	5.85	1.0	9.11	10	1.5	0.08	0.015	0.005	–
Mar M200	56.74	9	0.14	0.03	5	–	5.5	1.74	10	10	1.8	0.03	0.015	0.005	–
CMSX 4	61.7	6.5	–	0.6	–	6.5	5.6	1	9	6	0.1	–	–	–	3

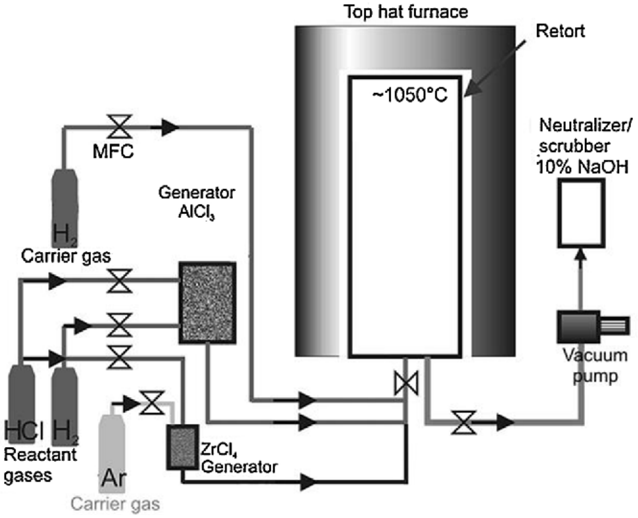

Fig. 1 – A scheme of equipment for deposition of aluminide coatings by the CVD method [22–27].

FIB type Dual Beam FEI [24–28]. Coatings' thickness was determined by means of the NIS-Elements software.

Oxidation tests of uncoated and coated samples were conducted at 1100 °C in the air atmosphere for 800 h. Samples were heated up to 1100 °C, kept at that temperature for 20 h and then cooled down in air to the room temperature for 1 h and then weighed with accuracy of 0.0001 g.

Phases of the aluminide coating before and after oxidation test were identified by X-ray diffraction (XRD). The surface analysis of bulk samples was performed. The ARL X'TRA X-ray diffractometer equipped with a filtered copper lamp with the voltage of 45 kV was used.

3. Results

The TEM investigation of an aluminide coating on pure nickel revealed its double-zone structure (Fig. 2). The average coating thickness is about 80 μm. The first zone, on the top of the coating, consists of the β-NiAl phase. The underlying, zone consists of the γ′-Ni$_3$Al phase. Digimap analysis confirmed the distribution of aluminum in both zones (Fig. 3).

The cross-section image (Fig. 4a) indicates, that aluminide coating deposited on Mar M247 superalloy consists of two layers: an additive layer (18 μm thick) and interdiffusion layer (20 μm thick) [25]. The EDS analysis of the additive layer showed, that the top, additive layer is composed of the β-NiAl phase (40 at.% Al, 49 at.% Ni) (Fig. 4b). The EDS analysis of the interdiffusion layer showed that it contains elements that diffused from the substrate (Fig. 4c). The surface of the aluminide coating is uniform as far as the chemical composition is concerned. It was established that aluminum content is 43 at.%, nickel 49 at.%, and cobalt 6 at.% Aluminum and nickel contents indicate the NiAl phase formation.

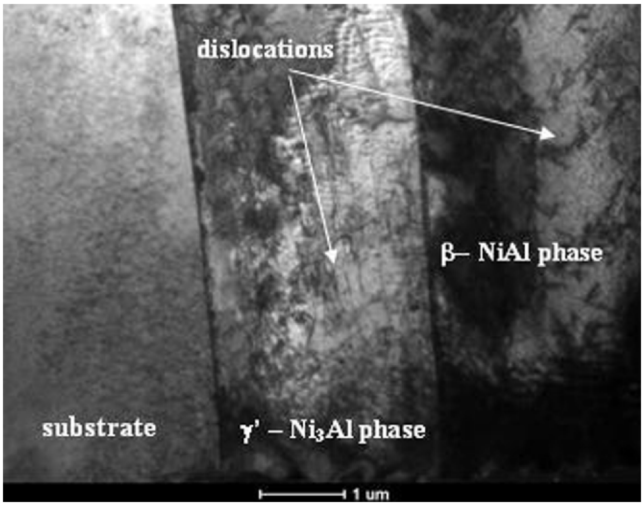

Fig. 2 – TEM micrograph of aluminide coating deposited on pure nickel.

As to reveal the phase composition of the inner zone, the gradual removal of the outer zone was performed by grinding. Then, the microstructure of the surface of the boundary of the outer and inner zone was observed (Fig. 5a). Homogenous areas (gray color) containing: Al – 35 at.%, Ni – 52 at.%, Co – 7 at.% and Hf – 0.6 at.% were observed. This chemical composition corresponds to the NiAl phase. Non-homogeneous areas (light color) containing 20% at hafnium were observed. The high hafnium content may lead to MC carbides formation. Some longitudinal precipitations enriched with Ta – 31 at.%, Ti – 27 at.%, W – 16 at.%, and Hf – 6 at.%, were revealed by the next gradual removal. This removal was performed to reveal the surface of the interdiffusion zone. Such elements form MC type carbides which are the microstructure constituents of

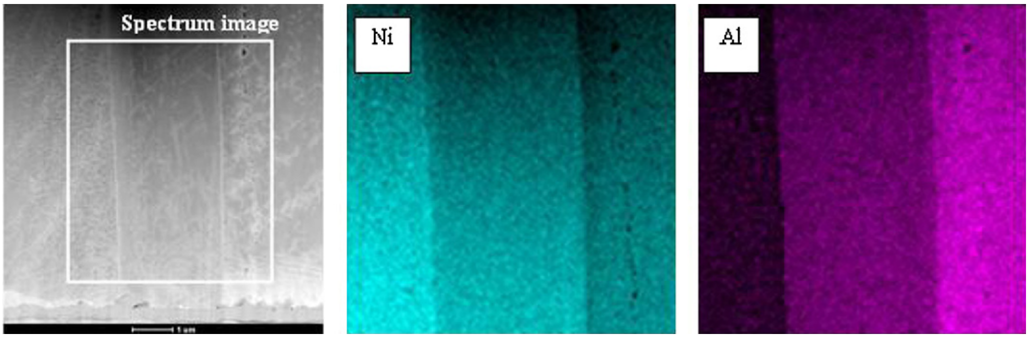

Fig. 3 – The digimap analysis of a aluminide coating deposited on pure nickel.

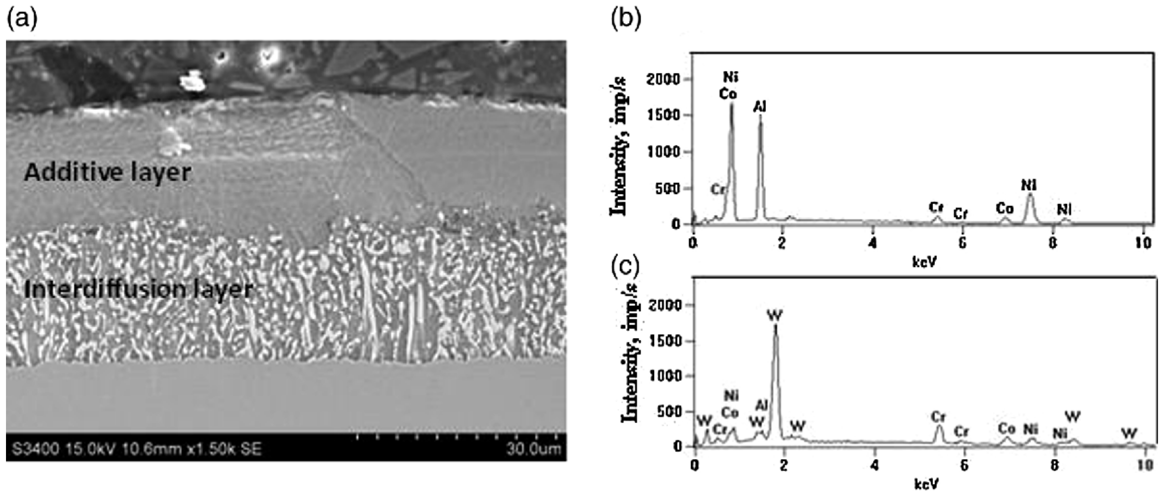

Fig. 4 – The cross-section microstructure of the aluminide coating deposited by the CVD method on Mar M247 (a), EDS spectrum of the additive layer (b) and EDS spectrum of the interdiffusion layer (c).

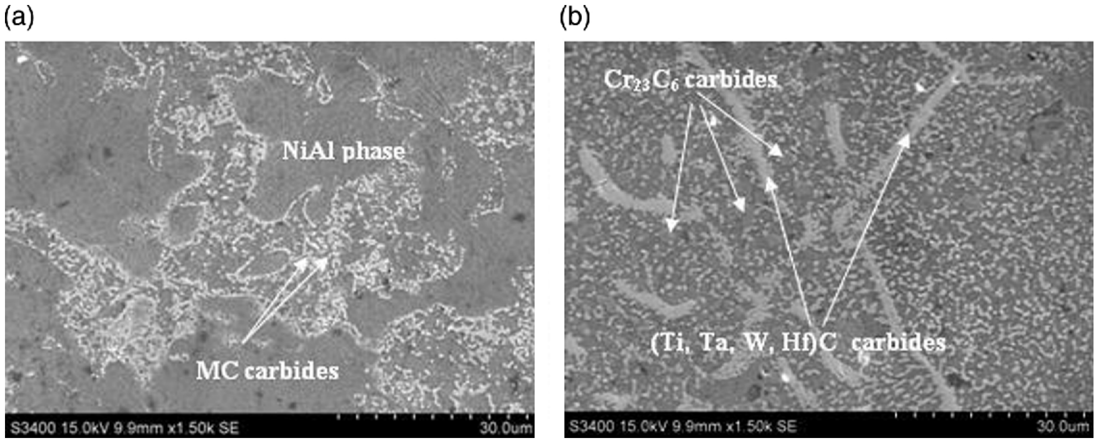

Fig. 5 – The microstructure of the interdiffusion layer of the aluminide coating deposited by the CVD method on Mar M247: on the boundary of the additive layer and the interdiffusion layer (a) and the interdiffusion layer (b).

Mar M247 superalloy (Fig. 5b). The fine, chromium enriched precipitates (Cr – 62 at.%) were found in the interdiffusion layer. Such large chromium content may lead to the $M_{23}C_6$ carbides formation [25].

The microstructure of aluminide coating deposited on Mar M200 is similar to the microstructure of the coating deposited on Mar M247 superalloy and consists of two layers: additive (20 μm thick) and internal (interdiffusion) one, (10 μm thick) (Fig. 6a–c). Additive layer comprises NiAl phase – (Al – 37 at.%, Ni – 53 at.%). The analysis of the chemical composition on the cross-section of the diffusion zone revealed the presence of aluminum (27 at.%), chromium (10 at.%), cobalt, nickel, titanium, hafnium and tungsten.

The cross-section of aluminide coating deposited on the CMSX 4 superalloy is presented in Fig. 7. The thickness of the coating was about 30 μm and a two-layer structure is observed (Fig. 7a–c). The additive layer is composed of Al – 44 at.%, Ni – 49 at.%, and small content of Co – 6 at.% and Cr – 4 at.% The surface of aluminide coating deposited on CMSX 4 substrate is more undulating than coatings deposited on Mar M247 and Mar M200 superalloys. This is due to higher undulating of CMSX 4 superalloy before aluminizing process.

The EDS analysis proved, that the top additive layer is composed of the β-NiAl phase. The EDS analysis showed, that the interdiffusion layer is composed of small (the size of less than a micrometer), round precipitates enriched with refractory elements (Cr – 12 at.%, Co – 13% at, W – 11% at and Re – 5% at). These elements form intermetallic compounds of a topologically close-packed structure in superalloys called a TCP phase [29]. Chen and Little [30] and Proctor [31] investigated the mechanism of TCP phases formation in CMSX 4 superalloy and proved, that the phase formed at 1050 °C is the μ-phase while the R phase is formed at 1150 °C. TCP μ-phase crystallizes in the rhombohedral crystallographic system, A_xB_y type structure. Thus, it may be assumed that $(W,Cr,Re)_x(Ni,Co)_y$ phases are formed in the interdiffusion layer.

X-ray diffractions confirmed that the additive layer of the coatings consists of the NiAl phase. Some peaks from $M_{23}C_6$

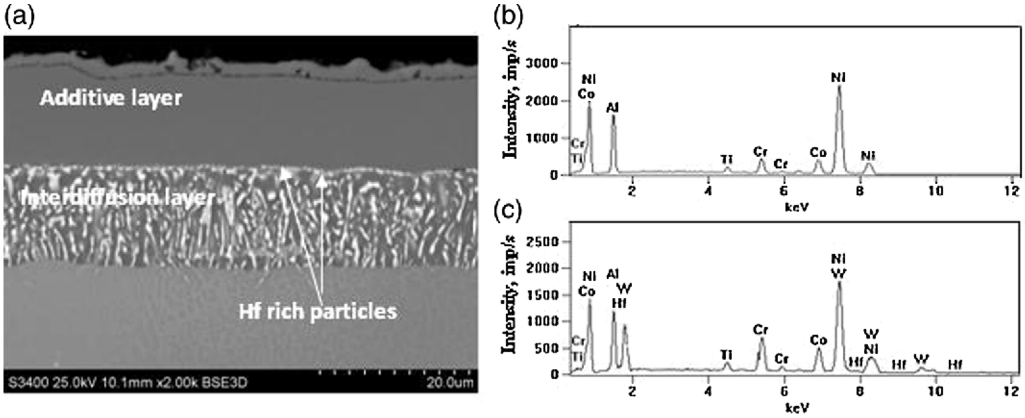

Fig. 6 – The cross-section microstructure of aluminide coating obtained by the CVD method on Mar M200 (a), EDS spectrum of the additive layer (b) and EDS spectrum of the interdiffusion layer (c).

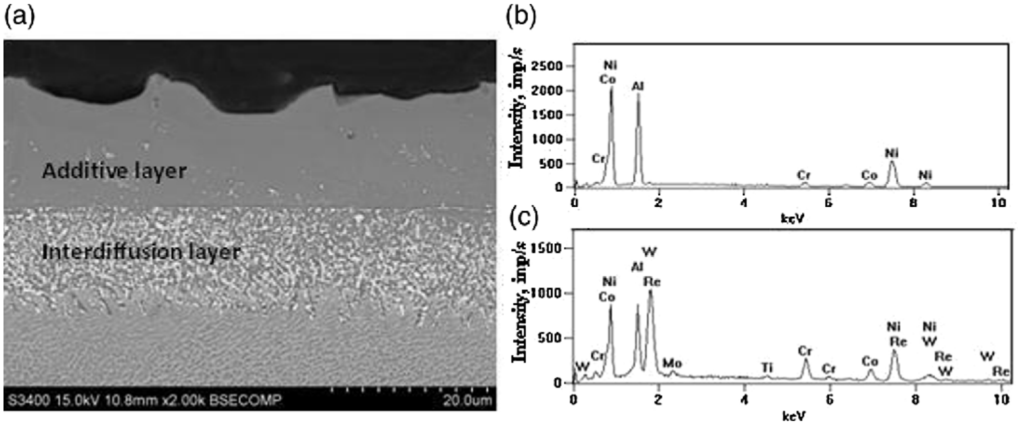

Fig. 7 – The cross-section microstructure of aluminide coating obtained by the CVD method on CMSX 4 (a), EDS spectrum of the additive layer (b) and EDS spectrum of the interdiffusion layer (c).

carbides appeared in coatings deposited on Mar M200 superalloy (Fig. 8).

The EDS analysis of the cross-section of the aluminide coating deposited on Mar M247 and Mar M200 superalloys showed that hafnium is situated 19 μm below the sample's surface (Fig. 9a and b). The EDS analysis on the cross-section of aluminide coating deposited on CMSX 4 superalloy does not indicate hafnium presence, but high rhenium content was observed in the interdiffusion layer (Fig. 9c and d). The EDS analysis of platinum modified aluminide coating was presented to compare oxidation resistance of the non-modified aluminide coating with the platinum modified aluminide coating (3 μm Pt) on CMSX 4 superalloy. It was found that platinum was distributed across the additive layer (Fig. 9d).

The results of oxidation test of coated and uncoated Mar M247 samples are shown in Fig. 10. The intensive mass losses appear just after 2 cycles of oxidation. The coated samples exhibit small mass gain.

After 5 cycles of oxidation aluminide coatings on Mar M247 substrate consisted of NiAl and Ni_3Al phases (Fig. 11). It was found, that outward aluminum diffusion occurs. Aluminum forms Al_2O_3 phase 3–4 μm thick, according to the following reaction: $NiAl + 3x/4O_2 \rightarrow NiAl_{1-x} + x/2Al_2O_3$. The inward diffusion of aluminum from the coating toward the substrate takes place [13]. Areas near boundaries of NiAl grains are depleted of Al, which indicates that grain boundaries of NiAl phase are easy paths for aluminum diffusion. The Ni_3Al phase is formed at the grain boundaries of NiAl, NiAl–Al_2O_3 phases and NiAl matrix. Chemical analysis after 5 cycles of oxidation revealed the presence of HfO_2 oxides surrounded by Al_2O_3 in the region called ''pegs''. Some authors [10,23,25] assume that pegs act as a diffusion barrier for substrate elements. The presence of reactive elements like Hf can change the growth mechanism from outward movement of aluminum ions to inward movement of oxygen ions [10,23]. Hafnium reduces aluminum content, necessary for the formation of a continuous protective alumina scale. HfO_2 oxides are formed on the grain boundaries of NiAl/Al_2O_3 phases. The presence of NiAl, Ni_3Al, Al_2O_3 and HfO_2 phases was confirmed by the XRD analysis (Fig. 12). Hafnium atoms like are located like zirconium in the Al sub-lattice of NiAl [17] and could contribute to faster annihilation of Al vacancies owing to their fast diffusion toward the coating/oxide interface and inhibit the formation and growth of cavities.

Two-phase oxide layer is formed after 40 cycles of oxidation. One mixture is $Al_2O_3 + HfO_2$ and the second one

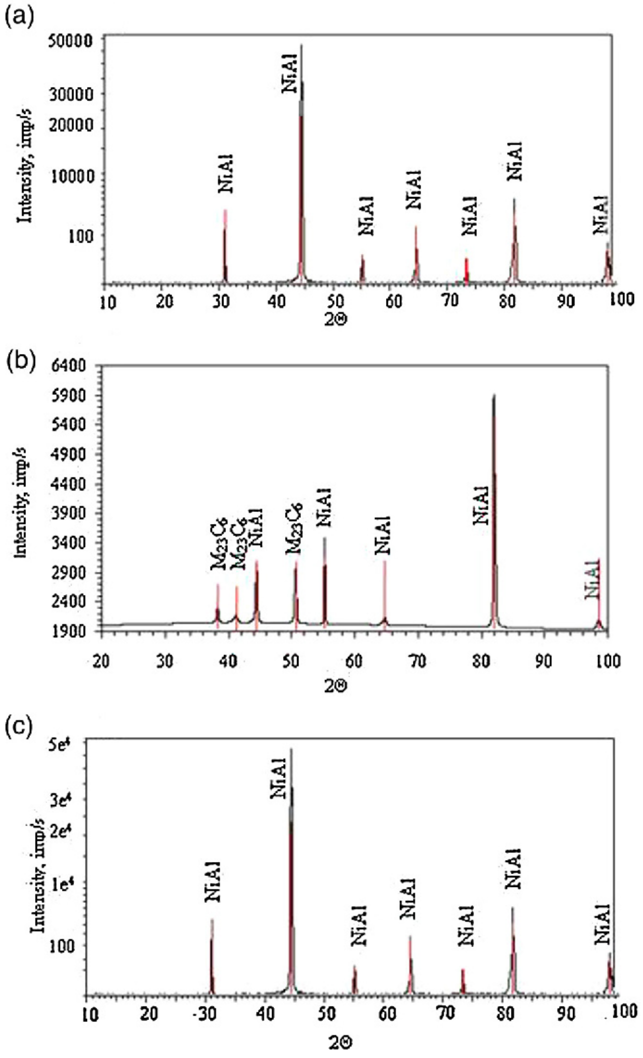

Fig. 8 – XRD pattern of the aluminide coating deposited by the CVD method on Mar M247 (a), Mar M200 (b) and CMSX 4 (c).

is $NiAl_2O_4 + Al_2O_3$ oxides' mixture. The aluminum content in the coating decreased with the prolongation of the oxidation time and after 1000 h dropped to 17 at.% in the outer zone and 9.6 at.% in the interdiffusion zone. There are still visible carbides enriched with Cr and W.

The results of oxidation test of coated and uncoated Mar M200 samples are shown in Fig. 13. The intensive mass losses are after 2 cycles of oxidation. The coated samples exhibit small mass gain. The oxidation process follows the parabolic rate law and provides a diffusion barrier of internal oxidation.

Hafnium-based oxide was observed in the scale formed after 40-cycles of oxidation at 1100 °C of the aluminide coating deposited on Mar M200 superalloy (Fig. 14a and b). Some NiO + Al_2O_3 + $NiAl_2O_4$ oxides' mixture was observed. The metallographic analysis of the cross-section proved, that the oxide scale is adherent to the substrate and consists of two layers (Fig. 15a and b). Digimap analysis of the coating after 40-cycles oxidation confirmed the presence of Hf-rich pegs at the oxide/coating interface (Fig. 16).

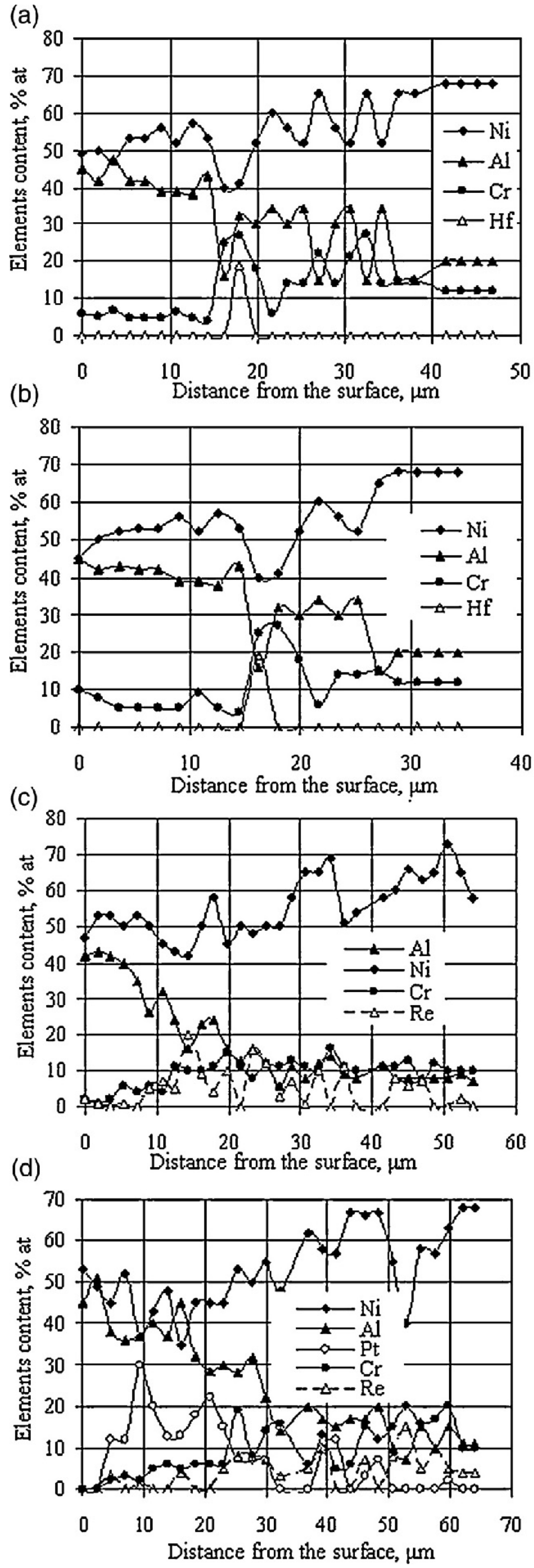

Fig. 9 – EDS analysis of the cross-section of aluminide coatings deposited on the Mar M247 (a), Mar M200 (b), CMSX 4 (c) and CMSX 4 + 3 µm Pt (d).

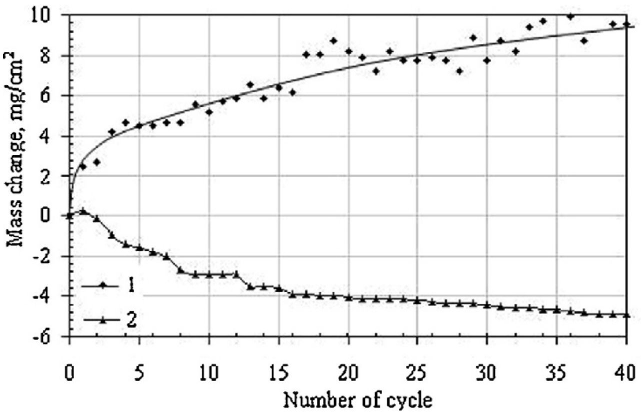

Fig. 10 – Mass change of Mar M247: (1) with aluminide coating and (2) without aluminide coating.

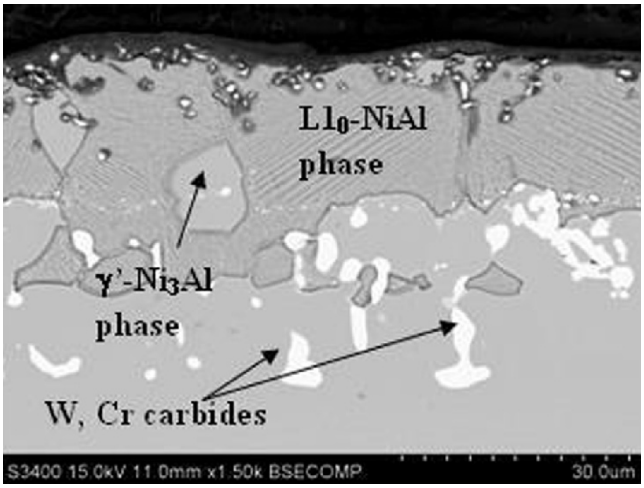

Fig. 11 – The microstructure of the cross-section of the aluminide coating deposited by the CVD method on Mar M247 superalloy after oxidation test at 1100 °C after 5-cycles of oxidation.

The oxidation curves of coated and uncoated CMSX 4 superalloy are presented in Fig. 17. The uncoated sample shows mass losses after 5 cycles of oxidation. A zero-cross-over in mass gain of aluminide coated CMSX 4 superalloy is observed after 8 cycles of oxidation. Platinum modification of aluminide coating (3 μm Pt) successfully protects CMSX4 substrate even to 40 cycles of oxidation.

The investigation of microstructure and chemical composition of aluminide layer deposited on CMSX 4 superalloy during oxidation at 1100 °C was presented in paper [29]. It was found that the aluminum content decrease in the β-NiAl phase after 6 cycles of oxidation. The Ni3Al phase was formed on the grain boundaries of the NiAl phase as a result of aluminum diffusion into the oxide layer. The change in morphology of intermetallic phases occurred in the diffusion zone. These phases are distributed on the depth of about 50 μm at an angle of 45° to the surface [29]. The prolongation of the oxidation time from 120 h to 354 h resulted in the growth of the surface layer roughness and $\gamma' \rightarrow \gamma$ phase transformation. The needle-like phases were observed after 20-cycles of oxidation at 1100 °C (Fig. 18a). The platinum modification of aluminide coating deposited on CMSX 4 superalloy was performed to increase the thermal stability of coated superalloy during oxidation. The β-NiAl phase was still observed after 20-cycles of oxidation of platinum modified aluminide coatings (Fig. 18).

4. Discussion

The presented results clearly show that aluminizing process succeeded throughout the procedure described within the experimental part. Aluminide coatings protect Mar M247, Mar M200 and CMSX 4 Ni-base superalloys against oxidation. Aluminizing at 1050 °C leads to formation of two layer coatings (additive and interdiffusion zones) both on pure nickel and nickel-based superalloys. In the case of pure nickel, a large

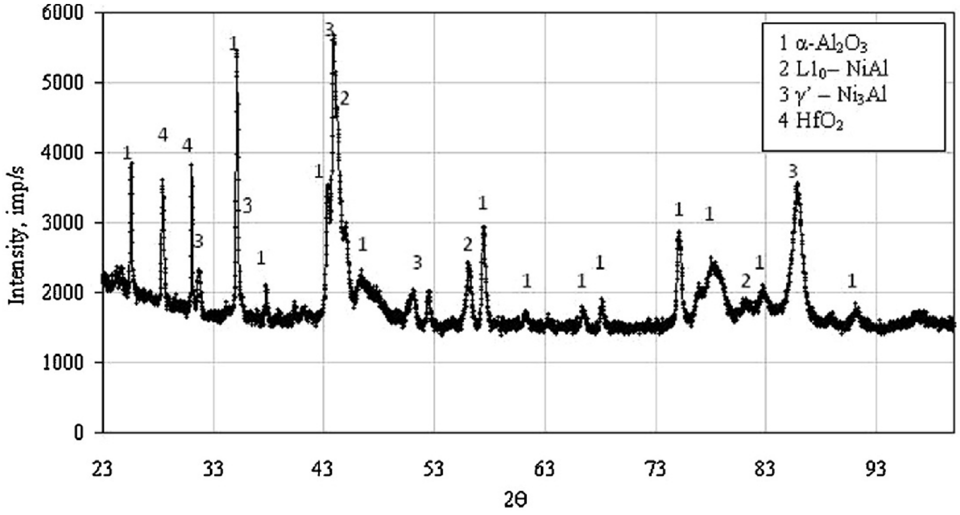

Fig. 12 – XRD pattern of the aluminide coating deposited by the CVD method after oxidation test at 1100 °C after 5-cycles of oxidation.

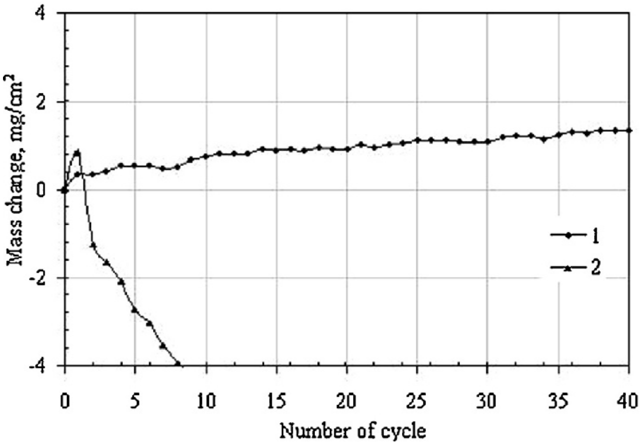

Fig. 13 – Mass change curves of Mar M200: (1) with the aluminide coating and (2) without the aluminide coating.

number of dislocation lines were observed in the additive zone, which is comprised of the NiAl phase and in the interdiffusion zone, which is consist of the Ni_3Al phase (Fig. 2). In the case of superalloys, additive zones are comprised of the NiAl phase, but interdiffusion ones are comprised of the NiAl phase and $M_{23}C_6$, MC carbides on the Mar M247 and Mar M200 superalloys and TCP phases on CMSX 4 superalloy. According to Nagaraj et al. [19] atoms of refractory elements are 'pushed' toward the substrate.

The NiAl phase in the microstructure of aluminide coating improves oxidation resistance of the substrate. Thermodynamically stable Al_2O_3 oxide is formed on the surface of aluminide coating during the oxidation test. The NiAl phase transforms into the Ni_3Al phase, of low oxidation resistance. This is due to aluminum diffusion from the coating to the Al_2O_3 oxide layer and the substrate. The Ni_3Al phase is formed on the boundaries of the NiAl grains, on the boundaries of NiAl/Al_2O_3 phases and NiAl/substrate. The increase of oxidation time causes Ni_3Al–Ni(Al) phase transformation and the decrease of oxidation resistance (weight loss observed on the oxidation curves).

Cooling of aluminide coatings from 1100 °C to room temperature results in a reversible martensitic transformation. Bose [32] alleges, that this type of transformation does not require diffusion but takes place by the coordinated displacement of atoms. The high-temperature B2 structure phase changes to the $L1_0$ phase. The morphology of the low-temperature martensitic phase is plate-like (Fig. 7). Several

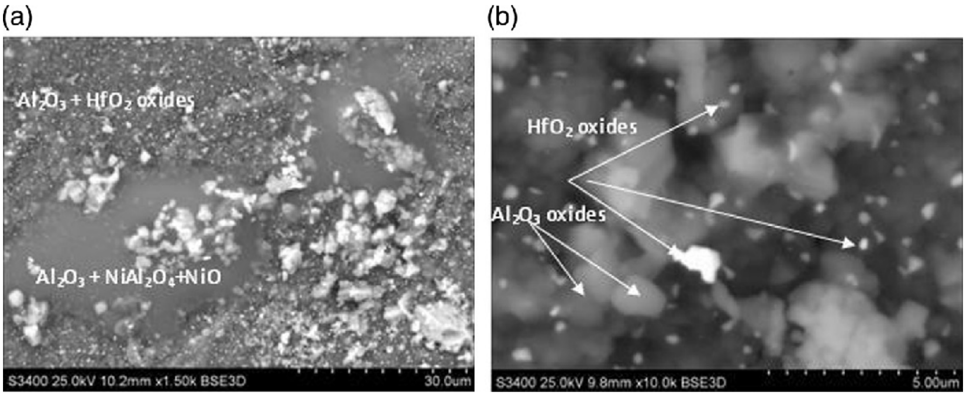

Fig. 14 – SEM morphologies of the aluminide coating deposited in the Mar M200 after oxidation at 1100 °C, Al_2O_3 + HfO_2 oxides and Al_2O_3 + $NiAl_2O_4$ + NiO oxides are visible (a), HfO_2 oxides are visible (b).

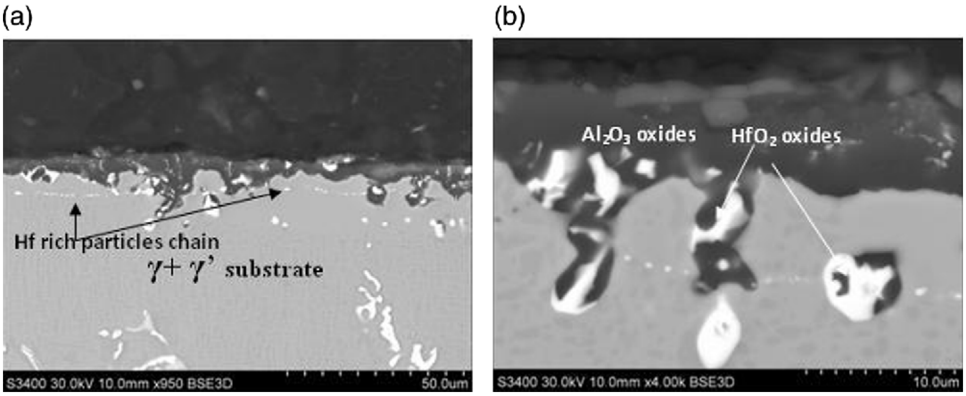

Fig. 15 – Microstructure of the cross-section of aluminide coating deposited by CVD method on Mar M200 after 40-cycles oxidation at 1100 °C.

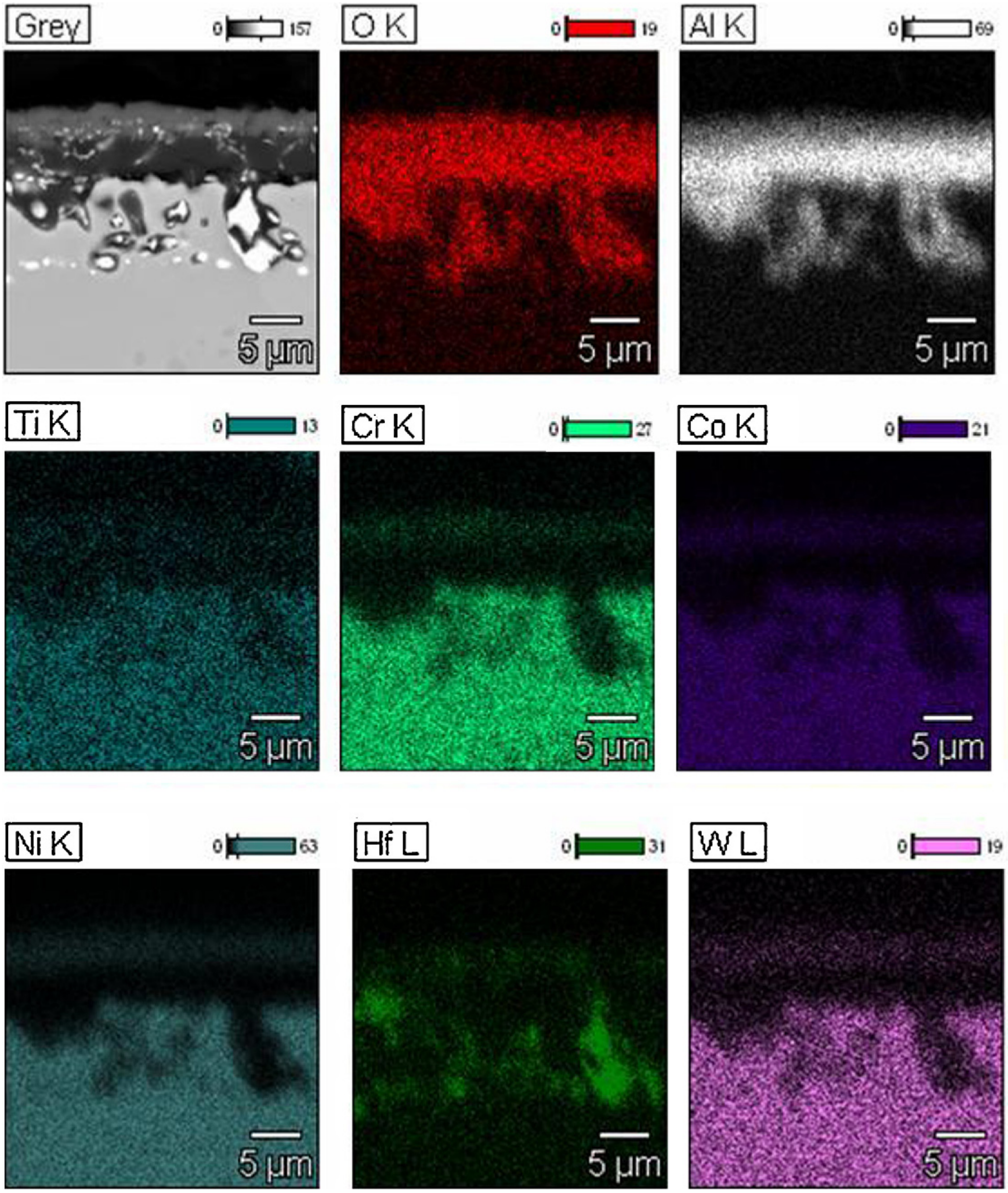

Fig. 16 – The digimap analysis of the aluminide coating deposited on Mar M200 after oxidation at 1100 °C.

conditions must be fulfilled for the martensitic transformation to occur. The aluminum content has to be less than 37 at.% and the coating needs to be exposed to the temperature about 1100 °C. It was assumed, that the temperature at which this transformation occurs depends on the Ni content and ranges between −200 and 900 °C. The martensitic transformation results in a volume change $\Delta V/V$ of approximately 2%, where V is the volume and ΔV is the change of volume.

It was proved, that oxidation resistance of coated Mar M247 and Mar M200 superalloys was better than coated CMSX 4 superalloy. It is due to hafnium presence in Mar M247 and Mar M200. Mar M247 superalloy contains 1.5 wt.% hafnium and Mar M200 – 1.8 wt.% hafnium, whereas CMSX 4 superalloy contains only 0.1 wt.% hafnium. Such small hafnium content in CMSX 4 Ni-base superalloy does not assure good oxidation resistance. The addition of hafnium to the Mar M247 and Mar M200 superalloys causes HfO_2 particles formation, so called 'pegs', in the Al_2O_3 scale. No pegs were observed in the Al_2O_3 scale on CMSX 4 superalloys. The 'pegs' presence in the oxides scale improved oxidation resistance. The formation of 'pegs' is due to the difference of oxygen diffusivity in HfO_2 and Al_2O_3 scales. The formation mechanism is probably as follows: Al_2O_3 scales are formed with embedded HfO_2 particles on hafnium-rich areas, such as grain boundaries [33,34]. Since the diffusivity of oxygen in HfO_2 is several orders of magnitude higher than in Al_2O_3, HfO_2 particles along Hf-rich grain boundaries acted as

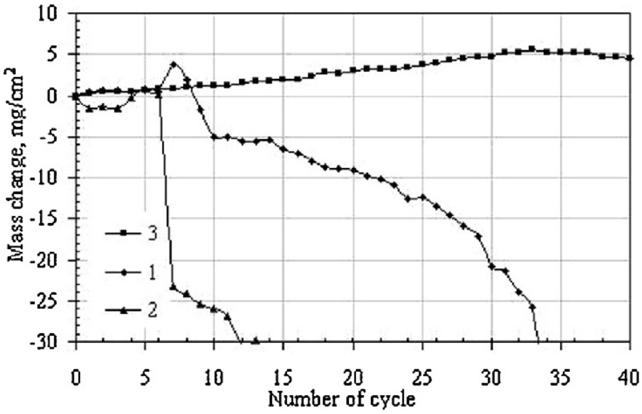

Fig. 17 – Mass change curves of CMSX 4: (1) with the aluminide coating, (2) without the aluminide coating and (3) with the platinum modified aluminide coating.

short circuit diffusion paths for oxygen transport, leading to preferentially localized scale thickening in the neighborhood of these particles, causing a deep penetration of the formed HfO_2 scales into the substrate [33,34]. The oxygen transported through this short circuit diffusion path reacts with Al atoms in the surrounding areas to form Al_2O_3 scales. Therefore HfO_2 'pegs' scales surrounded by Al_2O_3 scales are formed. High titanium (about 1 wt.%) and tantalum (about 6.5 wt.%) contents and low hafnium (0.1 wt.%) content in the CMSX 4 superalloy lead to less oxidation resistance of the aluminide coating in comparison to aluminide coatings deposited on Mar M247 and Mar M200 superalloys (Fig. 19).

Titanium and tantalum are scale components and have worse oxidation resistance than Al_2O_3 scale. To increase the oxidation resistance of aluminide coating deposited on CMSX 4 superalloy platinum modification (deposition of 3 μm thick platinum layer) was performed. Platinum incorporated in aluminide coatings allows the formation of pure Al_2O_3 oxide. Platinum decreases diffusion of alloying elements such as Ti and Ta from CMSX 4 substrate to the coating and oxide scale. Platinum stabilizes the NiAl phase in the coating and delays $NiAl \rightarrow Ni_3Al$ phase transformation.

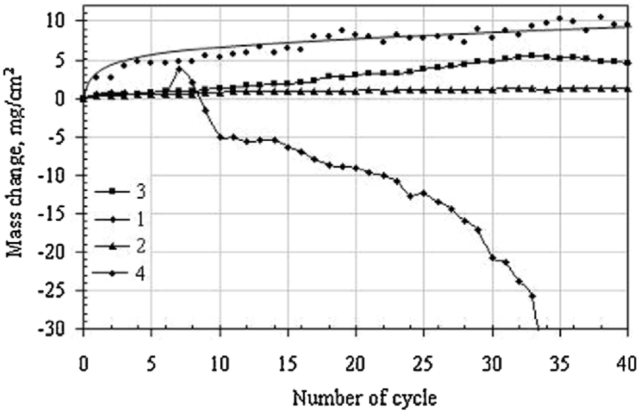

Fig. 19 – Mass change curves of the aluminide coatings deposited on: (1) CMSX 4, (2) Mar M200, (3) CMSX 4+3 μm Pt and (4) Mar M247.

5. Conclusions

Aluminizing by means of the CVD method leads to formation of two layers aluminide coatings deposited on nickel and nickel based superalloys. The additive – NiAl layer and the interdiffusion – Ni_3Al layer were formed after aluminizing of pure nickel.

The NiAl phase in the outer and interdiffusion zones was found after aluminizing of superalloys. Some $M_{23}C_6$ and MC carbides besides the NiAl phase were observed in the interdiffusion zone of aluminide coatings deposited on Mar M247 and Mar M200 superalloys. Topologically closed-packed phase was formed in the interdiffusion zone of aluminized CMSX 4 superalloy. Aluminized Mar M247 and Mar M200 superalloys exhibited a small mass increase and the α-Al_2O_3 scale was formed during the oxidation test. The α-Al_2O_3 scale had a good adherence to the coating. The presence of 1.5 or 1.8 wt.% hafnium in the substrate of aluminized superalloys leads to HfO_2 scales formation during oxidation The grain boundaries of NiAl and Al_2O_3 are the places of precipitation of HfO_2. Hafnium atoms could contribute to a faster annihilation of the aluminum vacancies owing to their fast diffusion

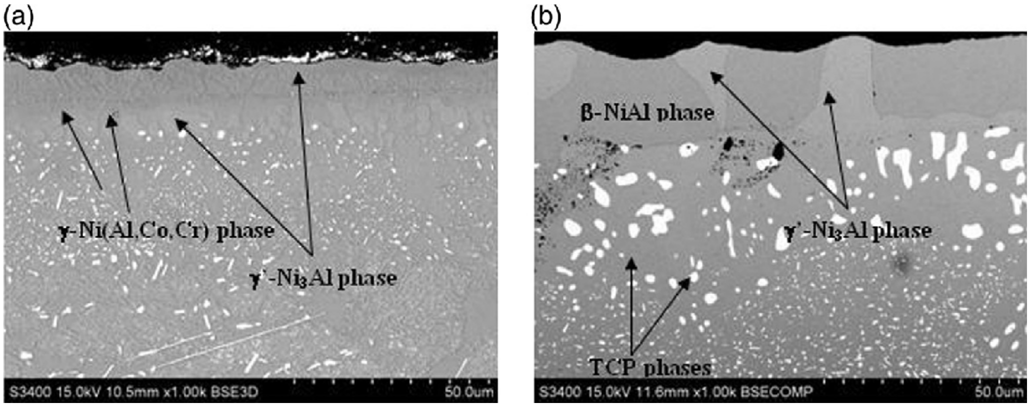

Fig. 18 – The microstructure of the cross-section of aluminide coating deposited by the CVD method on CMSX 4 after 20-cycles oxidation at 1100 °C: with the aluminide coating (a), with the platinum modified aluminide coating (b).

toward the coating/oxide interface and inhibit the formation and the growth of cavities. This phenomenon improves Al_2O_3 oxide spalling resistance during oxidation. The presence of small amount of hafnium (0.1 wt.%) and relatively high amount of titanium (1 wt.%) and tantalum (6.5 wt.%) in CMSX 4 superalloy is the reason of poor oxidation resistance of aluminized superalloy. Platinum modification of aluminide coatings deposited on CMSX 4 stabilized the NiAl phase, delayed NiAl → Ni_3Al phase transformation and decreased diffusion of alloying elements such as Ti and Ta from the substrate to the coating and oxide scales during oxidation [35].

Acknowledgment

The presented research was supported by the National Science Centre, Poland, project number 2011/01/B/ST8/05036.

REFERENCES

[1] N. Voudouris, Ch. Christoglou, G.N. Angelopoulos, Formation of aluminide coatings on nickel by a fluidised bed CVD process, Surface and Coatings Technology 141 (2001) 275–282.

[2] J.A. Haynes, Y. Zhang, K.M. Cooley, L. Walker, K.S. Reeves, B.A. Pint, High-temperature diffusion barriers for protective coatings, Surface and Coatings Technology 189 (2004) 153–157.

[3] M. Zagula-Yavorska, J. Sieniawski, T. Gancarczyk, Some properties of platinum and palladium modified aluminide coatings deposited by CVD method on nickel-base superalloys, Archives of Metallurgy and Materials 57 (2012) 503–509.

[4] M. Zagula-Yavorska, J. Sieniawski, Microstructural study on oxidation resistance of nonmodified and platinum modified aluminide coating, Journal of Materials Engineering and Performance 23 (2014) 918–926.

[5] J.A. Haynes, K.L. More, B.A. Pint, I.G. Wright, K. Cooley, Y. Zhang, High Temperature Corrosion and Protection of Materials, 5, 2000, . p. 35.

[6] Y. Niu, W. Wu, D. Boone, J. Smith, J. Zhang, C. Zhen, Oxidation behaviour of simple and platinum-modified aluminide coatings on IN738 at 1100 °C, Journal de Physique IV 3 (1993) 511–519.

[7] W.T. Griffiths, L.B. Pfeil, U.K. Improvement in heat-resisting alloys, Patent 459848 (1937).

[8] Y. Wang, M. Suneson, G. Sayre, Synthesis of hafnium modified aluminide coatings on Ni-base superalloys, Surface and Coating Technology 15 (2011) 1218–1228.

[9] B.A. Pint, I.G. Wright, W. Lee, Y. Zhang, B.A. Pint, I.G. Wright, W.Y. Lee, Y. Zhang, K. Prüßner, K.B. Alexander, Substrate and bond coat compositions: factors affecting alumina scale adhesion, Materials Science and Engineering A 245 (1998) 201–211.

[10] V.K. Tolpygo, K.S. Murphy, D.R. Clarke, Effect of Hf, Y and C in the underlying superalloy on the rumpling of diffusion aluminide coatings, Acta Materialia 56 (2008) 489–499.

[11] R. Tricot, Memoires et Etudes Scientifiques de la Revue de Metallurgie 88 (1991) 747.

[12] A.W. Cocchardt, W. Township, US Patent 3,005,705 (1961).

[13] B.M. Warnes, D.C. Punola, Clean diffusion coatings by chemical vapor deposition, Surface and Coatings Technology 94–95 (1997) 1–6.

[14] B.M. Warnes, Reactive element modified chemical vapor deposition low activity platinum aluminide coatings, Surface and Coatings Technology 146–147 (2001) 7–12.

[15] G.Y. Kim, L.M. He, J.D. Meyer, A. Quintero, J.A. Haynes, W.Y. Lee, Mechanisms of Hf dopant incorporation during the early stage of chemical vapor deposition aluminide coating growth under continuous doping conditions, Metallurgical and Materials Transactions A 35 (2004) 3581–3593.

[16] J.A. Nesbitt, B. Nagaraj, Pt and Hf addition to NiAl Bond Coats and their effect on the lifetime of thermal barrier coatings, The Minerals, Metals and Materials Society, 2001, pp. 79–92.

[17] S. Hamadi, M. Bacos, M. Poulain, A. Seyeux, V. Maurice, P. Marcus, Oxidation resistance of a Zr-doped NiAl coating thermochemically deposited on a nickel-based superalloy, Surface and Coating Technology 204 (2009) 756–760.

[18] B. Ning, M. Shamsuzzoha, M.L. Weaver, R.C. Bradt, Apparent indentation size effect in a CVD coated Ni-base superalloy, Surface and Coatings Technology 163–164 (2003) 112–117.

[19] B.A. Nagaraj, J.L. Williams, U.S. Patent 6,602,356 (2003).

[20] J. Restall, B. Gill, C. Hayman, N. Archer, A process for protecting gas turbine blade cooling passages against degradation, in: Superalloys, Metals Park, Ohio, 1980, pp. 405–411.

[21] J. Benoist, K.F. Badawi, A. Malie, C. Ramade, Microstructure of Pt-modified aluminide coatings on Ni-based superalloys, Surface and Coatings Technology 182 (2004) 14–23.

[22] M. Yavorska, J. Sieniawski, M. Zielińska, Functional properties of aluminide layer deposited on inconel 713 LC Ni-based superalloy in the CVD process, Archives of Metallurgy and Materials 56 (2011) 187–192.

[23] M. Zielińska, J. Sieniawski, M. Yavorska, M. Motyka, Influence of chemical composition of nickel based superalloy on the formation of aluminide coatings, Archives of Metallurgy and Materials 56 (2011) 193–197.

[24] J. Romanowska, M. Zagula-Yavorska, J. Sieniawski, Zirconium influence on microstructure of aluminide coatings deposited on nickel substrate by CVD method, Bulletin of Materials Science 36 (2013) 1043–1048.

[25] M. Zielińska, M. Zagula-Yavorska, J. Sieniawski, R. Filip, Microstructure and oxidation resistance of an aluminide coatings on the nickel based superalloy Mar M247 deposited by CVD aluminizing process, Archives of Metallurgy and Materials 58 (2013) 697–701.

[26] M. Zagula-Yavorska, J. Morgiel, J. Romanowska, J. Sieniawski, Nanoparticles in zirconium-doped aluminide coatings, Materials Letters 139 (2015) 50–54.

[27] J. Romanowska, Aluminum diffusion in aluminide coatings deposited by the CVD method on pure nickel, Computer Coupling of Phase Diagrams and Thermochemistry 44 (2014) 114–118.

[28] A. Nowotnik, J. Sieniawski, M. Zawadzki, M. Goral, The effect of long-term annealing on microstructure of aluminide coatings deposited on MAR M200 superalloy by CVD method, Key Engineering Materials 477 (2014) 592–593.

[29] M. Yavorska, J. Sieniawski, Thermal stability of microstructure of aluminide layer deposited by CVD method on CMSX 4 nickel base superalloy, Materials Science Forum 674 (2011) 89–96.

[30] J.H. Chen, J.A. Little, Degradation of the platinum aluminide coating on CMSX4 at 1100 °C, Surface and Coatings Technology 92 (1997) 69–77.

[31] C.S. Proctor, Department of Materials Science and Metallurgy, (Ph.D. thesis), University of Cambridge, 1994.

[32] S. Bose, High Temperature Coatings, Burlington, 2007.

[33] Y. Wang, M. Suneson, Synthesis of Hf-modified aluminide coatings on Ni-base superalloys, Surface and Coatings Technology 206 (2011) 1218–1228.

[34] H. Hindam, D.P. Whittle, Microstructure, adhesion and growth kinetics of protective scales on metals and alloys, Journal of the Electrochemical Society 5/6 (129) (1982) 245–284.

[35] F. Pedraza, Implications of diffusion on the composition and microstructures of platinum modified aluminide coatings on CMSX 4 single crystal superalloys, Defect and Diffusion Forum 289–292 (2009) 277–284.